

Aconitase

**A quick peek into the spectroscopic determinations behind its
bioinorganic structure and mechanism**

Alper Sarikaya

Chemistry 419 - University of Washington

June 11th, 2008

Introduction to Aconitase

Aconitase (citrate [isocitrate] hydrolase, EC 4.2.1.3) is one of the earliest studied proteins that involve a cubical [4Fe-4S] inorganic cluster to catalyze the stereospecific isomerization of its substrate. Though [4Fe-4S] clusters typically function as part of elaborate electron transport chain, aconitase is unique in that instead of facilitating a long electron transport chain, it seems to use the electron density of the delocalized cluster to help coax the stereospecific change of citrate. Aconitase proves to be an integral part of the Krebs cycle (also known as the citric acid cycle) that is an integral part of cellular respiration - the presence of aconitase is abundant in the mitochondria of all aerobic cells. As this cycle is such a vital part of biological systems, it is an important mechanism to understand completely.

Aconitase serves the double-purpose of both hydration and dehydration of constituents of the Krebs cycle, effectively creating a stable

intermediate, *cis*-aconitic acid. By catalyzing the dehydration of citrate to *cis*-aconitate

and the stereospecific hydration of *cis*-aconitate

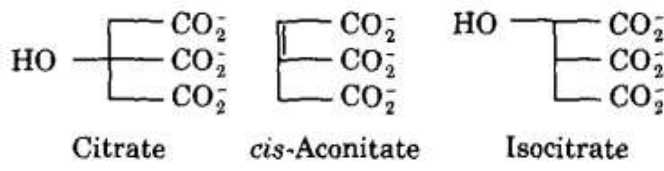


Figure 1 - The compounds involved in aconitase catalysis

to isocitrate, the enzyme effectively performs two functions to perform the interconversion of citrate to isocitrate^{1-5,7}. More specifically, the catalysis is from citrate to 2R, 3S-(+)-isocitrate, with the stereospecificity proven by model compounds². Aconitase therefore facilitates the removal of H₂O for the first step and re-addition of H₂O for the second, protecting its substrate from the surrounding aqueous solvent through a hydrophobic exterior.

The structure of aconitase is very curious as it was one of the first [4Fe-4S] clusters discovered in Nature but strangely is one of the only of such proteins that directly interacts with the substrate to induce a change. To be catalytically active, the protein must have ferrous ions available². The reason for this will become clear later in the paper; the short of it is that the iron [4Fe-4S] cluster must have four iron ions –

the cluster will relax to three iron ions if there is an iron deficiency^{6,7}. The iron cluster itself is coordinated by several cystine residues, without which the efficacy of the enzyme drops tenfold. The pH optimum of aconitase is in the alkaline range, which is in agreement with reduction and oxidation behavior of the enzyme³.

Something that is curious about aconitase is the fact that it uses iron as the inorganic substituent. Mutagenic studies on aconitase have found substituting the iron ions with nickel ions allow the active site to be easier to crystallize, but the substitution renders aconitase completely inactive. Similar to nickel, substitution of the iron ions with manganese also renders aconitase inactive, but unlike nickel its substitution is thermodynamically favored – and therefore manganese is poisonous in this respect^{2,3}. Early on, Villafranca and Mildvan were able to detect the presence of substrate-Fe(II)-enzyme ternary complex at the active site of aconitase via ¹H NMR⁴. By using the Fe(II)-activated form of the enzyme in the present of citrate in a solution of D₂O at a pH of 7.5, Villafranca and Mildvan were able to pinpoint the ¹H coupled with the Fe and were able to determine that iron is the primary metal. It was not until detailed Mössbauer spectra outlined the presence of multiple iron ions that the scientific community realized the presence of the [4Fe-4S] cluster⁶⁻⁸. The iron ion on its own is destructive to the cell, producing free radicals as well as damage to lipids, other proteins, and DNA. As a result, the metabolism of iron must be tightly controlled as to never release an iron ion into the mitochondrial matrix – we see that this is indeed true as Fe-S bonds are greatly activated, but never fully broken⁵.

Past Work – Structure Determinations and Mechanisms

Research on aconitase stretches back to the mid 1950s where aconitase was isolated as part of the Krebs cycle. In 1958, Gawron *et al.* gained insight into the degree of stereospecificity of *cis*-aconitase¹. By using various model compounds such as isocitric acid and alloisocitric acid, it was determined that there exists a repeatable *trans* mechanism for the reversible dehydration of isocitric acid, implying a

trans mechanism for the reversible dehydration of citric acid as well. From this determination, Gawron *et al.* surmised that the alpha-hydrogen of these substrates does not participate in the role of aconitase mechanism as the *trans* mechanism is nowhere near the proximity of the changing subunit. Additionally, the authors found that there was a common intermediate in the reversible dehydration/hydration of isocitrate and citrate: *cis*-aconitic acid. Gawron *et al.* saw that the addition of a water molecule to the bound substrate could produce either isocitrate or citrate while generating a proton. From this, the authors surmised that the mechanism is thusly a reversible 'acid-catalyzed' hydration of the double bond and that the initial proton comes from a water molecule bound to a substrate-Fe(II)-aconitase complex (EMS, or enzyme-metal-substrate) that was the most popular simplification of the mechanism at the time.

Villafranca and Mildvan several years later in 1972 admit that the evidence is convincing for EMS complexes, as suggested by earlier stereospecific studies combined with the high (or absolute) specificity for Fe(II) and proton relaxation studies of water with a aconitase-manganese-substrate bridge complex⁴. Classified as type II enhancement, Villafranca and Mildvan have found that the catalytically inactive aconitase-Mn(II) complex will bind the substrate as well as water. Though the authors admit a surmounting pile of evidence, they acknowledge that this data does not completely prove that there is a simple EMS complex in play for aconitase, and set out to do ¹H NMR studies to gain more insight. Through their NMR studies of Fe(II)- and Mn(II)-aconitase with both citrate and *trans*-aconitate substrate attached, Villafranca and Mildvan determined the rough structures of the substrate bound to the metal, using crystallographic data from Gabe, Glusker *et al* and Dargay, Glusker *et al* to support their findings.

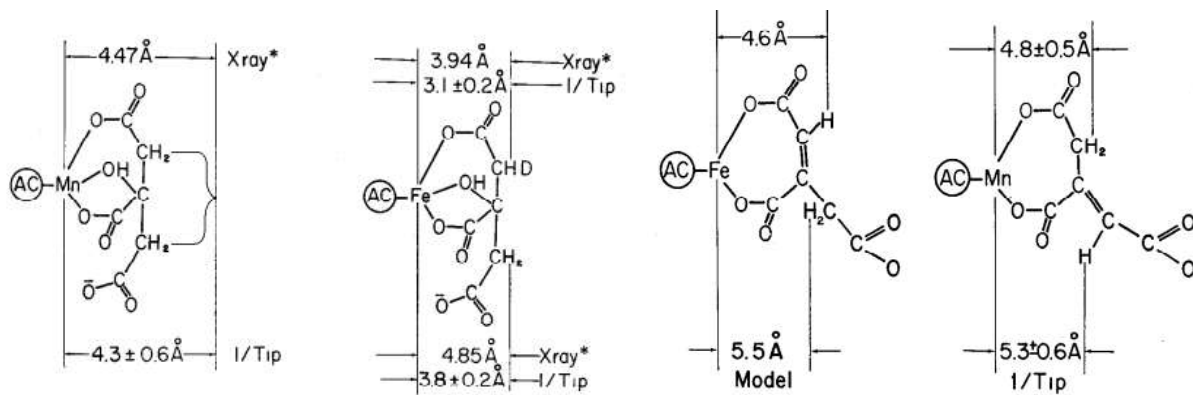


Figure 2 - Two pairs of NMR-inferred structures (on left) and their crystallographic comparisons (on right).⁴

Given these characterizations of the molecules, Villafranca and Mildvan composed a mechanism with three different intermediate paths. For the isomerization of citrate to isocitrate to be facilitated, either the substrate or the ligands attached to the iron ion must rotate to accommodate the stereospecific transformation. Although the end result is the same for all paths, there are three separate mechanisms to get them to that point (Fig. 3). The first is the ferrous wheel mechanism (Fig. 3, steps 2a and 2b) that involves breaking of a metal-ligand bond, specifically the C-3 *cis*-aconitate carboxyl group, to allow the six-coordinated iron to rotate into such a position to rehydrate the substrate. Similarly, the reverse ferrous wheel mechanism (Fig. 3, steps 3a and 3b) also requires a bond disconnection but instead temporarily cleaves a water molecule. The last intermediate path has been coined the name of “bailar twist”, named after John C. Bailar, Jr., an inorganic chemist who investigated the rotational process. By rotating the rear three ligands but not the front three, the Bailar twist mechanism can accommodate the rotation without necessitating the temporary breakage of bonds, making it an attractive choice.

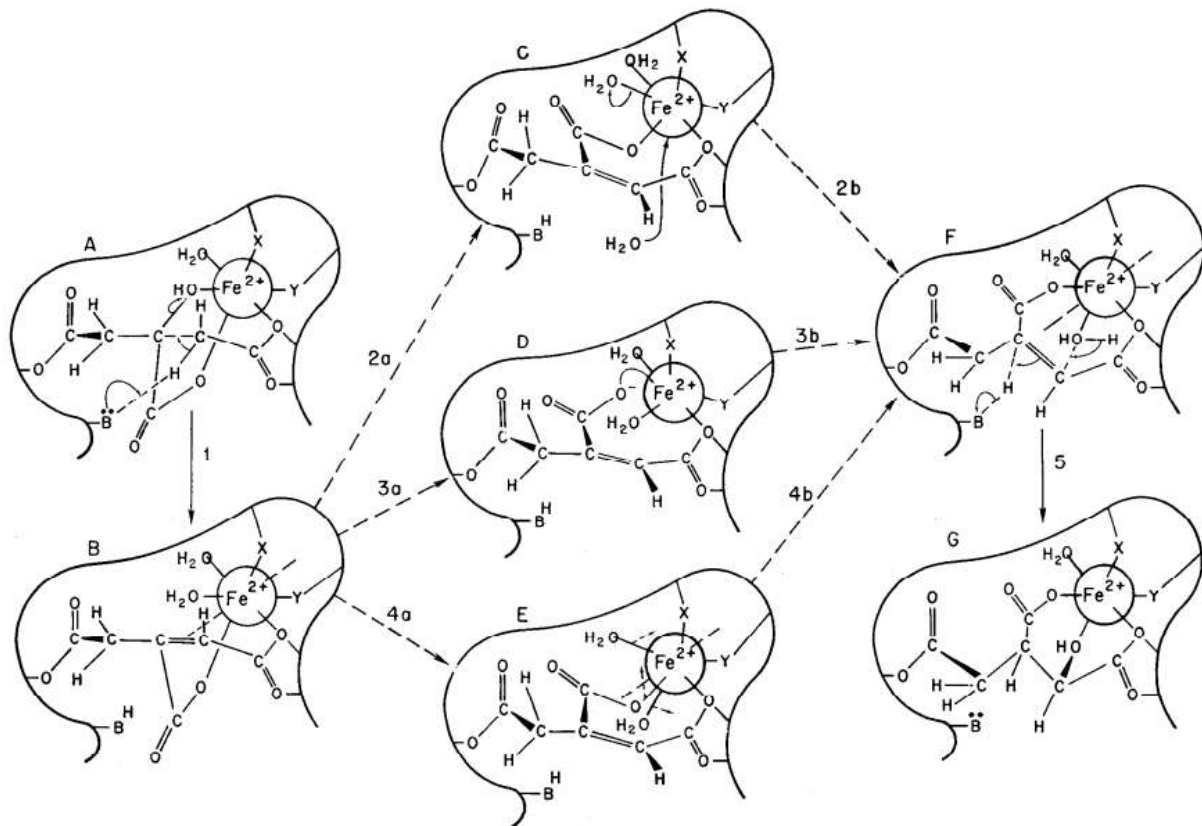


Figure 3 - Three alternative mechanisms for the conversion of citrate to isocitrate catalyzed by aconitase. From the elimination of water (Step 1) to form the *cis*-aconitate intermediate, the substrate can follow either of three pathways (Steps a, b). The broken line on intermediate 4 highlights the 3-fold axis about which the Fe^{2+} performs the Bailar twist. Finally, water adds to form isocitrate (Step 5).⁴

The Bailar twist is further appealing as it has been described previously to occur within $\text{Fe}(\text{II})$ complexes with soft π bonding ligands such as sulfur. (This historical perspective becomes important as we can see the pieces of this puzzle falling into place!) However, at that time, there was insufficient evidence to rule out any of the three mechanistic paths.

Aconitase – Characterization of the Metal Site

Making use of visible, electron paramagnetic, and Mössbauer studies, Emptage *et al.* identified the various states of the [4Fe-4S] cluster and their redox states⁶. First, by oxidative titration of aconitase by ferricyanide, the authors ascertained that there were no detectable intermediates between active

aconitase [4Fe-4S] (upper spectrum) and inactive aconitase [3Fe-4S] (lower spectrum), shown by the smooth transition between the two (Fig. 4) Secondly, Emptage *et al.* performed optical analysis as shown at lower left (Fig. 5), displaying the four stable states of the iron complex in aconitase. The reduced aconitase $[3\text{Fe-4S}]^{1+}$ is represented in curve A and a further photoreduced cluster $[3\text{Fe-4S}]^0$ is shown by curve B. To obtain the spectra for the activated cluster, the authors added Fe^{2+} and dithiothreitol to obtain the $[4\text{Fe-4S}]^{2+}$ activated cluster for curve C, and further photoreduced the complex to obtain $[4\text{Fe-4S}]^{1+}$ for curve D. The significance of these curves is that they are clear and distinct from one another, allowing for segmentation and classification of these different oxidation states.

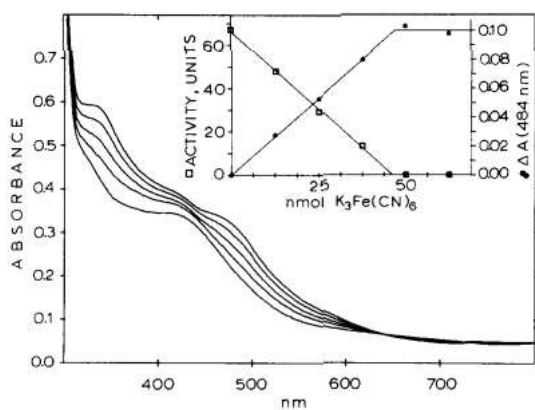


Figure 4 - Oxidative titration of active aconitase with potassium ferricyanide followed by spectrophotometry.⁶

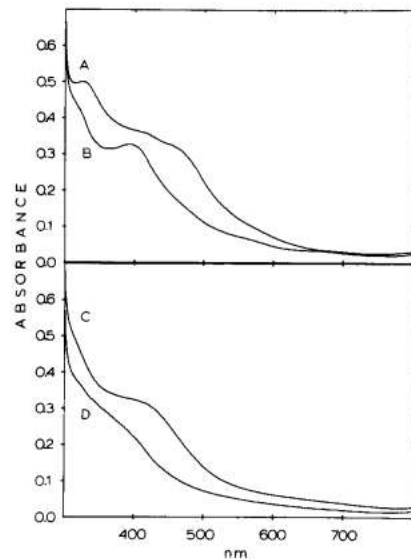


Figure 4 - Optical spectra of the four stable states of aconitase. (A) is inactive aconitase, (B) is just (A) with photoreduction, (C) is activated aconitase, and (D) is (C) with photoreduction.⁶

The spectra start to get more interesting as we move on to electron paramagnetic resonance (EPR) spectroscopy; Emptage *et al.* were among the first to discover the effect of substrate on the aconitase iron cluster's oxidation state. Important to note here is that both the inactive form $[3\text{Fe-4S}]^0$ and the active form $[4\text{Fe-4S}]^{2+}$ are both EPR-silent as they have an even number of spin electrons – this problem is skirted by using $[4\text{Fe-4S}]^{1+}$ active aconitase which only differs by its efficiency at reactivity (70% less

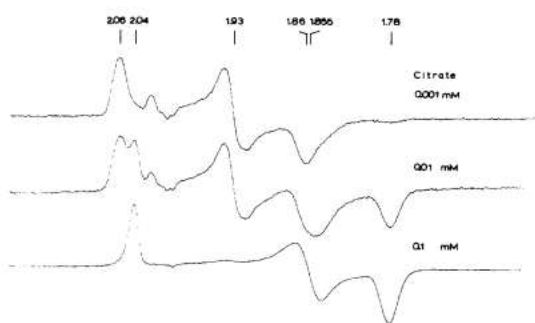


Figure 6 – Activated aconitase (5.0 mg/mL). Citrate for this experiment were photoreduced for 10 min in an anaerobic EPR tube and quickly frozen with liquid nitrogen. Temperature: 13 K, microwave power: 0.9 mW, modulation: 0.8 mT, microwave frequency: 9.24 GHz.⁶ Notice the three spectra in terms of citrate added.

reactive than its $[4\text{Fe}-4\text{S}]^{2+}$ counterpart⁷). By taking $[4\text{Fe}-4\text{S}]^{1+}$ aconitase without a substrate, they found it in the inactive form as shown as the top-most graph (Fig. 6), with an isotropic signal at $g = 2.01$ – confirming the presence of a 3Fe cluster. By gradually adding an amount of citrate, Emptage *et al.* find that the EPR peaks shift upfield from 2.06, 1.93, 1.86 to 2.04, 1.85, 1.78, all characteristic of $[4\text{Fe}-4\text{S}]^{1+}$ clusters. While this

information gives us a quick peek at tracing electron spins and substrate-derived ligands and is strengthens the assumptions made from other spectra, the EPR spectra does not stand on its own and requires additional data from ENDOR, Mössbauer, and resonance Raman to solidify the exact structure of the iron cluster⁷.

From their studies, Emptage *et al.* were able to characterize the four separate stable states of aconitase and diagram their relationships between Fe-S cluster type, activity, and oxidation state. The authors condense the four states into two-word phrases: oxidized inactive, reduced inactive, oxidized active, and reduced active. There are several distinctive features of each which are outlined in the table below.

	Oxidized Inactive	Reduced Inactive	Oxidized Active	Reduced Active
Iron cluster	$[3\text{Fe}-4\text{S}]^{1+}$	$[3\text{Fe}-4\text{S}]^0$	$[4\text{Fe}-4\text{S}]^{2+}$	$[4\text{Fe}-4\text{S}]^{1+}$
Optical spectra	Shoulder at 484nm	Broad peak at 395nm	Shoulder at 410nm	-
EPR	Isotropic $g = 2.01$	EPR-silent	EPR-silent	$g = 1.94$
Found <i>in vivo</i>	Yes	Yes	Yes	No

Some aspects of this characterization to note: reduced inactive aconitase was initially difficult to isolate as it scavenged Fe^{2+} from the surrounding solution and quickly transforms into a $[4\text{Fe}-4\text{S}]$ cluster. Luckily, this is easily inhibited by EDTA, presumably by the mechanism that chelates the extraneous iron efficiently enough to prevent activation. This most definitely shows the thermodynamic favorability *in*

vivo of aconitase when there is excess iron in the mitochondrial matrix. For the oxidized active form of aconitase to become inactive, it must be in a reducing environment, implying that there should be a $[4\text{Fe}-4\text{S}]^{3+}$ counterpart that serves as the intermediate between the oxidized active and the oxidized inactive forms of aconitase. However, this intermediate has not been isolated yet and Emptage *et al.* left it as uncertain (Fig. 7, highlighted by the parenthesis around the complex). The reduced active form of aconitase is not found *in vivo* due to its decreased amount in activity, but is immensely useful in the characterization studies of $[4\text{Fe}-4\text{S}]$ clusters as it is EPR-active while its *in vivo* counterpart, oxidized active aconitase, is not.

Mössbauer spectroscopy has been one of the most informative techniques in elucidating the exact structure of the $[4\text{Fe}-4\text{S}]$ cluster as it allows direct viewing of the Fe ions and discrimination between them. By looking at the structure of reduced inactive aconitase ($[3\text{Fe}-4\text{S}]^0$) and looking at the isomer shifts for each iron in both of the active states (+2 and +1), some clarifications to the exact structure and mechanism (!) are made. The Mössbauer spectra at right (Fig. 8) shows the reduced inactive state and how the electron is delocalized over the cluster. As stated before, addition of EDTA is necessary to isolate the reduced inactive state and its spectra is displayed first (A). The second graph (B) is the actual graph of the $[3\text{Fe}-4\text{S}]$ cluster with the irons labeled as ^{57}Fe ; the two quadrupole doublets are visible here in a 2 to 1 ratio, indicating that two ions of iron have more

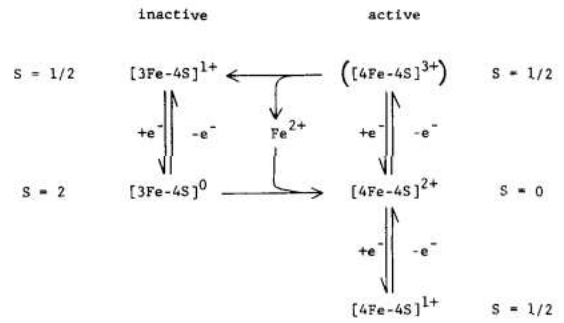


Figure 5 – A model describing the relationships between various forms of the aconitase Fe-S cluster. Note that the $[4\text{Fe}-4\text{S}]^{3+}$ is in parenthesis because its existence is questioned.⁶

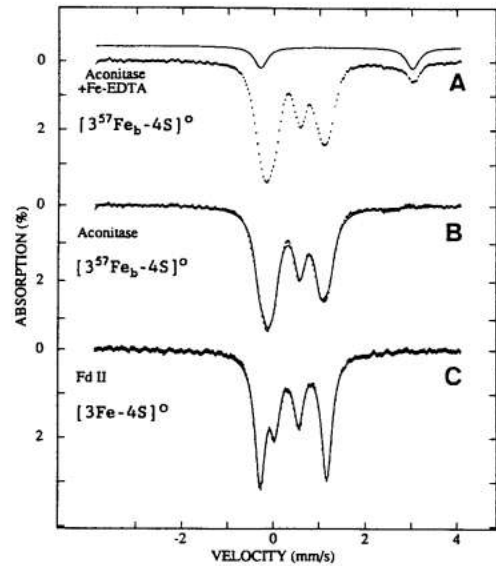


Figure 6 – Mössbauer spectra of the $[3\text{Fe}-4\text{S}]^0$ cluster of aconitase and ferredoxin II of *Desulfovibrio gigas*.⁷

ferrous (Fe(II)) character than the other and therefore take on the extra electron while the remaining iron ion is distinctly ferric (Fe(III)). While the doublets overlap in the low-velocity limit for aconitase, another iron cluster-containing compound named ferredoxin II (derived from *Desulfovibrio gigas*) is shown as a comparison. Ferredoxin II's low-velocity doublets are separated as opposed to aconitase's overlap.

Immensely important observation here comes from closer observation of both of the active forms. When the Mössbauer isomer shifts of Fe ions are collected for the active forms, we get the data on the left. The most notable fact is the isomer shift increase of the Fe_a ion between substrate binding and the idle active state. Fe_a falls into the range of high-spin ferrous complexes (0.7 mm/s – 1.4 mm/s), while the remaining three seem to form a localized (or ‘trapped’) valence. The repercussion of these observations are two-fold; (1) the advancement of the Fe_a atom to a high-spin ferrous state gives it the opportunity to become a pentacoordination or hexacoordination atom through relatively high d-electron density as compared to the rest of the Fe ions in the cluster, and (2) the protein environment must be such as to allow this non-symmetric transition to occur – a perception that I’ve already hinted at with the stabilization created by cystine residues stabilizing the Fe_{b1-3} ions. Two caveats that must be kept in mind, however, are that these measurements are made at very low temperatures (around 2 K) and may not represent its room temperature counterpart and that

[4Fe-4S] charge	Configuration	Isomer Shift
2+	Aconitase	0.45 (Fe_{a} , Fe_{b1-3})
2+	Aconitase + sub	0.84-0.89 (Fe_a) 0.45 (Fe_{b1-3})
+	Aconitase	0.65 (Fe_a)
+	Aconitase + sub	1.00 (Fe_a)
+		0.64 (Fe_{b1})
		0.49 ($\text{Fe}_{b2,3}$)

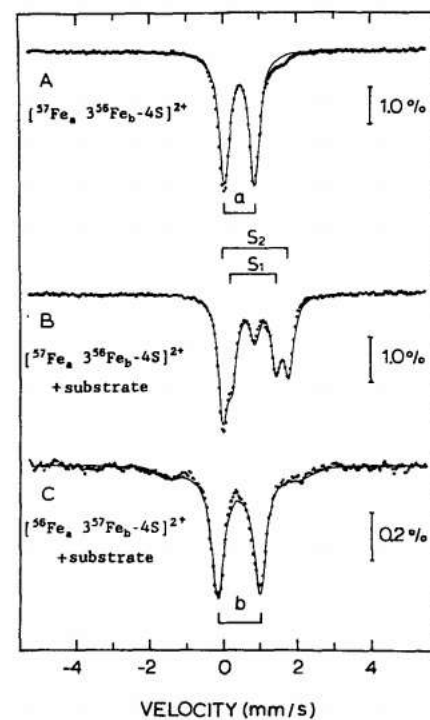


Figure 7 – Mössbauer spectra of the [4Fe-4S]²⁺ cluster of aconitase with (B and C) and without (A) substrate.⁷

the sulfur atoms involved in the iron cluster cannot be detected by Mössbauer and could also be changing their electron density as well. For completeness, the Mössbauer spectra corresponding to the above table is shown at right. (A) is simply the oxidized active form of aconitase without a substrate – we can see that all iron ions are at about the same oxidation state. In (B), the Fe_a ion has been labeled as ^{57}Fe and substrate has been added – the result is increased isomer shift and quadrupole splitting. For (C), the other iron ions have been labeled as ^{57}Fe and there is no distinct, discernable difference between (A) and (C).

Insofar there has not been much exploration into the actual ligand coordinating environment of the Fe_a ion as the main concentration was on structural determination of the iron cluster. Electron-nuclear double resonance or more commonly abbreviated ENDOR satisfies this discrepancy by making it possible to look at the non-protein ligands of Fe_a and the actual binding sites of the substrate. ENDOR also permits probing the exchangeability of protons and ligation of the solvent to the paramagnetic center. By using differently labeled solvents $^1\text{H}_2\text{O}$ and $^2\text{H}_2\text{O}$, we can see the effect that the solvent has on the active site by taking the difference. In the ^1H -ENDOR spectra on the next page (Fig. 10), graph (A) is aconitase with no substrate in $^2\text{H}_2\text{O}$, (B) is the graph of aconitase with *cis*-aconitate in $^2\text{H}_2\text{O}$, and graph (C) represents aconitase with citrate in $^1\text{H}_2\text{O}$. It is uncertain how to assign the protons in (A) as they could be from protons of the Cys ligands or even the His101, 147, 167 ligands. For (B) we can see a slight deviation from (A) but it is clear that the non-bonding hydrogens in *cis*-aconitate are not involved in the mechanism as there was no change in the spectra of (B) between normal and deuterated *cis*-aconitate. There is, however, a large difference between (B) and (C) with a change of solvent from $^2\text{H}_2\text{O}$ to $^1\text{H}_2\text{O}$, the most notable of which is the signal of a highly-coupled proton at $A = 7.8$ MHz. Since the hyperfine coupling is large, Beinert and Kennedy assigns the proton signal to a cluster-bound H_xO ($x = 1,2$) based on their previous work⁸.

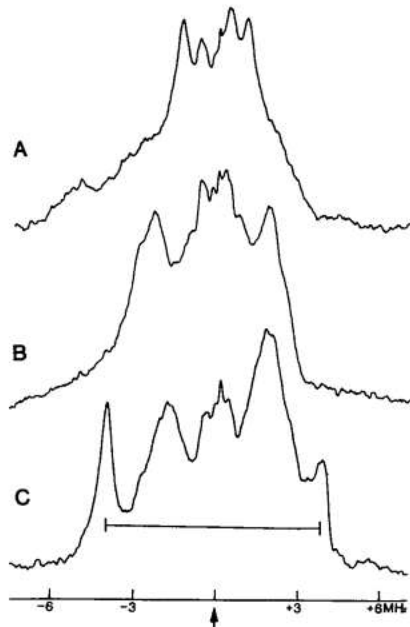


Figure 9 – ^1H -ENDOR spectra of $[4\text{Fe}-4\text{S}]^+$ cluster of aconitase without substrate (A), with deuterated *cis*-aconitase (B), and with citrate (C). The solvent is $^2\text{H}_2\text{O}$ for (A) and (B); the solvent is $^1\text{H}_2\text{O}$ for (C). Temperature is 2 K.⁷

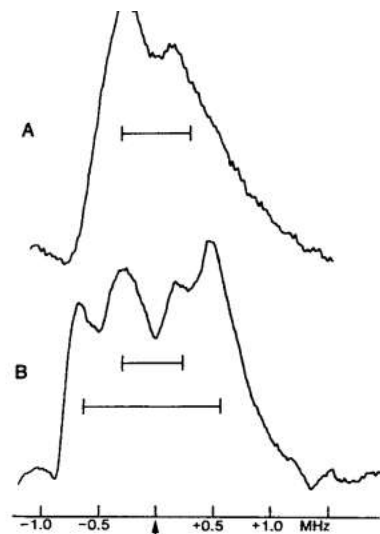


Figure 8 – ^2H -ENDOR spectra of the $[4\text{Fe}-4\text{S}]^+$ cluster of aconitase in the presence (B) and absence (A) of substrate.⁷

In order to further characterize the solvent species H_xO , Beinert and Kennedy took a ^2H -ENDOR spectra of aconitase in the absence (A) and presence (B) of substrate in $^2\text{H}_2\text{O}$. The enzyme-substrate complex shows two doublet signals at $\text{A}_1(^2\text{H}) = 1.2 \text{ MHz}$ and $\text{A}_2(^2\text{H}) = 0.5 \text{ MHz}$. By multiplying A_1 by the ratio of the nuclear g values predicts hyperfine coupling of $\text{A}_1(^1\text{H}) = 7.8 \text{ MHz}$, precisely what was determined by the previous ^1H -ENDOR spectra, confirming the presence of a cluster-bound H_xO . Doing a similar transformation on A_2 , $\text{A}_2(^1\text{H}) = 3.25 \text{ MHz}$ is obtained, a peak that is highly obscured with other non-exchangable proton resonances in the previous ^1H -ENDOR spectra. Based on these two observations of these two distinct protons, the authors conclude that this mystery H_xO ligand must be H_2O . Through ^{17}O -ENDOR measurements, Beinert and Kennedy have also found that substrate-free aconitase also binds a solvent H_xO species. Similar to the above case, $\text{A}(^1\text{H}) = 4 \text{ MHz}$ and $\text{A}(^2\text{H}) = 0.6 \text{ MHz}$ are directly related, but unlike the above, there is no ^2H doublet present, suggesting the presence of a hydroxyl ion iron ligand.

^{13}C , ^{57}Fe , ^{33}S , and ^{14}N ENDOR spectra were also taken of the active site of aconitase, but did not yield any novel information. Much of the insinuation from the taken spectra had been known for at least a decade from ^1H NMR and early EPR studies.

Kilpatrick, *et al.* took several resonance Raman (RR) spectra a couple years later in 1994, and found a

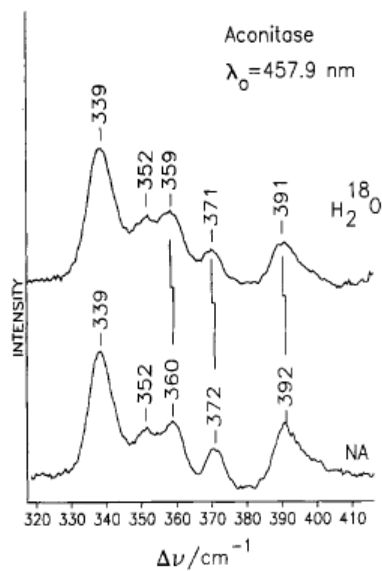


Figure 12 – RR spectra (77 K) of natural abundance (NA) and H_2^{18}O -equilibrated aconitase. 457.9 nm, 100mW laser, 4-cm^{-1} slit widths.⁹

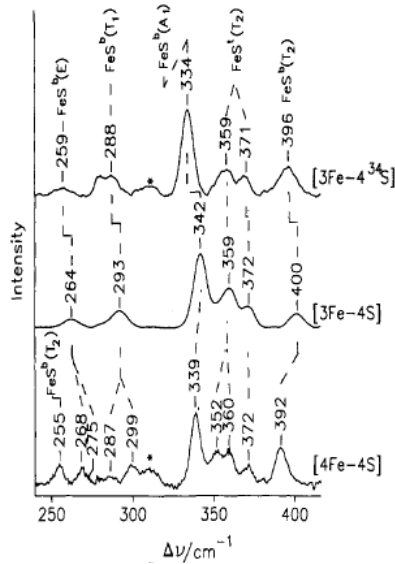


Figure 13 – RR spectra (77 K) of $[3\text{Fe}-4\text{S}]^+$ inactive aconitase and $[4\text{Fe}-4\text{S}]^{2+}$ active aconitase. The former was excited at 488.0 nm, while the latter was excited at 457.9 nm.⁹

mountain of supporting evidence for all the conclusions drawn before them and also gained a profound insight into the hydrogen-bonding of the [4Fe-4S] cluster.⁹ Initially, they studied the effects of aqueous solvent on the active site of aconitase. As the reader should know by now, regardless of whether substrate is bound, there is a hydroxyl group bound to the Fe_a ion. By taking the RR spectra at left (Fig. 12), the authors found very little difference between the two – there is only a slight shift in Fe-S vibrations from the H_2^{18}O and the enzyme in its natural environment. The aconitase Fe-OH stretches cannot be directly detected here, but by looking at the shift of the Fe-S stretch, we can get some clues to what is occurring in these two environments. The small downshifts of the highest-frequency Fe-S modes signify the vibrational mixing of Fe-S with Fe-O bonds, reaffirming the conclusions drawn from earlier spectroscopic measurements. Similarly, an RR spectra displaying both the active and inactive forms of aconitase ([4Fe-4S] vs [3Fe-4S]) justifies previous conclusions. In the spectra at left (Fig. 13), we can see again that there is not too much difference between the spectra – though the subtle aspects matter! Here, we see that some peaks in the

lower region vanish when moving from the active to the inactive form, mostly in the 250-300 cm⁻¹ range. As well as vanishing upfield Fe-S peaks, almost all of the downfield Fe-S peaks shift downfield. The reasoning for this is due to the loss of the Fe_a ion – three Fe-S bonds are lost. As the bonds are broken, the remaining Fe-S bonds rearrange themselves to thermal and kinetic equilibrium, falling into vibrational modes at lower frequencies. The top-most spectra is similar to that of [3Fe-4S], except for the ³⁴S used instead of naturally-occurring sulfur. For hydrogen bonding, peaks are similarly assigned based on known values of C-C-N, C=O, and Fe-S stretches.

Conclusions, Future Work

The enzyme of aconitase is in a unique group of bioinorganic proteins that have been essentially fully characterized and extensively studied. From Gawron *et al.* in 1958 realizing the stereospecificity of the catalysis performed by aconitase to the present-day characterization of the cubic [4Fe-4S] cluster *in vivo*, this protein has been subjected to many studies yielding compatible spectroscopic data, leading to involved scientific discourse between all parties. The structure of the active site and organic-ligating substituents are all known, the mechanism has been finalized, and the protein itself has been sequenced for some time now. It is known from ⁵⁷Fe ENDOR and ¹H NMR that the citrate/isocitrate hydroxyl, a solvent H₂O, and the terminal carboxylic acid all bind to the Fe_a ion while the enzyme is active. From ³³S ENDOR, EPR, and resonance Raman studies, it is known that three cystine residues stabilize the cluster: Cys 358, Cys 424, and Cys 421, among other protein ligands that give hydrogen-bonding character. Beinert, Kennedy, and others have discovered via Mössbauer and ENDOR that there is some sort of trapped valence of the iron ions in the cluster, highlighted by the fact that the four Fe atoms in the activated form are not equivalent. Due to this unique setup by Nature, aconitase does not facilitate its purpose by utilizing the electron-transport capabilities exhibited by so many other enzymes containing

the iron [4Fe-4S] cluster – aconitase instead uses the high electron density of the cluster to coax the hydroxyl group, resulting in the stereospecific isomerization of citrate to isocitrate.

Although from first glance there seems to be not much more to discover here, aconitase exists in slightly different forms in different organisms. While all aerobic organisms utilize the Krebs cycle (and therefore aconitase) in the mitochondria to enable cellular respiration, it seems that there is some sort of evolutionary staple that is left on each one.⁵ Since aconitase responds so violently to oxidation (quickly moving from the active form to the inactive form), many biochemists have turned their studies toward studying aconitase and the mitochondrial environment surrounding it *in vivo* rather than further chemical characterizations.

¹ Gawron, O., Glaid, A. J. III, LoMonte, A., Gary, S. *J. Biol. Chem.*, **1958**, *80*, 5856-5060

² Strouse, J., Layten, S. W., Strouse, C. E. *J. Am. Chem. Soc.*, **1977**, *99*, 562-572

³ Strouse, J. *J. Am. Chem. Soc.* **1977**, *99*, 572-580

⁴ Villafranca, J. J., Mildvan, A. S. *J. Biol. Chem.*, **1972**, *247*, 3454-3463

⁵ Brown, N. M., Kennedy, M. C., Antholine, W. E. & Eisenstein, R. S. *J. Biol. Chem.*, **2002**, *277*, 7246-7254

⁶ Emptage, M. H., Dreyer, J.-L., Kennedy, M. C., & Beinert, H. *J. Biol. Chem.*, **1983**, *258*, 11106-11111

⁷ Beinert, H. & Kennedy, M. C. *Eur. J. Biochem.*, **1989**, *186*, 5-15

⁸ Telser, J., Emptage, M. H., Merkle, H., Kennedy, M.C., Beinert, H. & Hoffman, B. M. *J. Biol. Chem.*, **1986**, *261*, 4840-4846

⁹ Kilpatrick, L. K., Kennedy, M. C., Beinert, H., Czernuszewicz, R. S., Qiu, D. & Spiro, T. G. *J. Am. Chem. Soc.* **1994**, *116*, 4053-4061